COMMUNICATION SCIENCES

AND

ENGINEERING

XI. OPTICAL PROPAGATION AND COMMUNICATION

Academic and Research Staff

Prof. Robert S. Kennedy
Prof. Jeffrey H. Shapiro
Prof. Cardinal Warde
Dr. Horace P. H. Yuen

Graduate Students

Steven L. Bates
M. Yousoff Burmawi
Samuel J. Dolinar, Jr.
Richard R. Gillock
Jeffry R. Long
Jesús A. Machado Mata
Paul Moroney
Nam-Soo Myung
Woo Hyun Paik
David M. Reilly
Warren S. Ross
Steven V. Sperry
Raymond J. Staron
Mahmoud Tebyani

A. OPTICAL COMMUNICATION IN THE ATMOSPHERE AT MIDDLE ULTRAVIOLET WAVELENGTHS

JSEP

Joint Services Electronics Program (Contract DAAB07-75-C-1346)

Robert S. Kennedy, Horace P. Yuen

An experimental and theoretical investigation of atmospheric optical communication at wavelengths in the 0.22-0.29 μm region was initiated last fall. It is motivated by the absence of background noise in this region and by the availability of low-noise detectors at these wavelengths.

These factors are very important in the realization of improved all-weather performance for they allow the realization of quantum-limited operation, even in the presence of severe scattering. Thus the performance is limited primarily by the total energy in the receiver field of view and by the coherence bandwidth (or time dispersion) of this energy. To the extent that these are not severely affected by the presence of multiple scattering, a communication system operating at these wavelengths will not be severely affected by low visibility (scattering) conditions.

The initial effort has been to set up a propagation experiment that can monitor the received energy levels. The system terminals are now complete and have just been put into operation. The transmitter is a low-pressure mercury vapor discharge generating approximately 1 W CW at 0.2537 μm in an uncollimated pattern. For ease of detection, it is square-wave modulated at 60 Hz. The receiver employs an RCA 4522 PMT operated with a gain of 10^7. It is preceded by chemical and dielectric filters and followed by an up-down photoelectron counter. The collecting area of the receiver is 10^{-2} m^2 and its field of view can be as large as 2π sr (full hemisphere). During the period of initial adjustment, the system has been operated over a 600 m path. That distance may be increased subsequently to magnify the effects of multiple scattering.

To complement the experimental program, a theoretical study of propagation in scattering atmospheres has also been initiated. Since the fields are expected to be

JSEP

JSEP quite incoherent, a photon scattering formulation of the transport equation is being employed. The quantities to be determined are the received energy level and coherence bandwidth as functions of the receiver field of view for various atmospheric conditions and operating ranges. JSEP

B. EXACT SOLUTION OF ULTRASHORT PULSE PROPAGATION IN A TWO-PHOTON MEDIUM

National Aeronautics and Space Administration (Grant NGL 22-009-013)

Horace P. Yuen, Flora Y. F. Chu

A novel pulse-shortening behavior in traveling-wave two-photon amplification has been exhibited recently for long pulses.[1] In this report we show that for this same simple model of a resonant two-photon medium in either the amplifier or the attenuator configuration, unlimited pulse sharpening occurs for ultrashort pulse propagation, in direct contrast with the one-photon case.[2,3] The results are derived from the exact global solution of the propagation equations for an arbitrary initial pulse shape. This exact solution describes the complete behavior of the pulse propagation in a simple analytic manner, also in contrast with the one-photon case where only asymptotic results are generally available.[2-6]

Consider a homogeneously broadened two-photon medium of identical two-level atoms with energy separation $2\hbar\omega$ so that each atomic transition gives rise to the absorption or emission of two photons at the same frequency ω.[7] The equations governing the propagation of plane-wave ultrashort pulses in the usual slowly varying envelope approximation are

$$\frac{\partial \mathscr{E}}{\partial z} = -\frac{\gamma}{2c}\mathscr{E} - i\frac{2\mu}{c}\mathscr{E}^*\mathscr{M} \tag{1}$$

$$\frac{\partial \mathscr{M}}{\partial \tau} = i\mu\mathscr{E}^2 D \tag{2}$$

$$\frac{\partial D}{\partial \tau} = i2\mu(\mathscr{M}\mathscr{E}^{*2} - \mathscr{M}^*\mathscr{E}^2) \tag{3}$$

where $\tau = t - z/c$ so that (z, τ) are the coordinates moving with velocity c. The variables $\mathscr{E}$ and $\mathscr{M}$ are the complex envelopes for the electric field and atomic polarization, D is the population difference between the upper and the lower levels, μ is a real positive two-photon coupling coefficient with μ^2 proportional to the two-photon absorption coefficient σ_A, and $1/\gamma$ is the photon lifetime in the medium. Equations 1-3 follow from the model of Yuen,[1] which gives more precise definitions of the variables. (The units of the variables in the present traveling-wave case are on a per unit volume basis, with σ_A in units of cm^4-s and μ in units of cm^3/s.)

We restrict ourselves, for simplicity, to the "constant phase" case and let $\mathscr{E} = E$ and $\mathscr{M} = -\frac{i}{2} M$ be real so that Eqs. 1-3 with $P \equiv E^2$ become

$$\frac{\partial P}{\partial z} = -\frac{\gamma}{c} P - \frac{2\mu}{c} PM \tag{4}$$

$$\frac{\partial M}{\partial \tau} = -2\mu PD \tag{5}$$

$$\frac{\partial D}{\partial \tau} = 2\mu PM. \tag{6}$$

Equations 5 and 6 imply the conservation law

$$D^2 + M^2 = \text{constant}. \tag{7}$$

The medium at $z \geq 0$ is excited by a pulse $P_o(t)$ starting from $t = t_o$,

$$D(z, t_o) = D_o, \quad M(z, t_o) = 0, \quad P(0, \tau) = P_o(\tau). \tag{8}$$

From (7) and (8),

$$D(z, \tau) = D_o \cos \psi, \quad M(z, \tau) = -D_o \sin \psi. \tag{9}$$

We define

$$P(z, \tau) = \frac{1}{2\mu} \frac{\partial \psi}{\partial \tau}, \quad \psi \equiv 2\mu \int_{t_o}^{\tau} P(z, t)\, dt, \tag{10}$$

and Eq. 4 gives

$$\frac{\partial^2 \psi}{\partial z \partial \tau} = \left(-\frac{\gamma}{c} + g \sin \psi\right) \frac{\partial \psi}{\partial \tau}. \tag{11}$$

The sign of the gain parameter $g \equiv 2\mu D_o/c$ depends on D_o,

$$g < 0 \text{ for } D_o < 0 \text{ (attenuator)}$$

$$g > 0 \text{ for } D_o > 0 \text{ (amplifier)}. \tag{12}$$

Equation 11, after integration with respect to τ, yields

$$\frac{\partial \psi}{\partial z} = -\frac{\gamma}{c}\psi + g(1-\cos\psi), \tag{13}$$

from which an "area theorem" follows immediately:

$$\frac{d\theta}{dz} = -\frac{\gamma}{c}\theta + g(1-\cos\theta), \qquad \theta(z) \equiv \psi(z,\infty). \tag{14}$$

Equation 13 can be solved exactly for $\gamma = 0$:

$$\psi(z,\tau) = 2\cot^{-1}\left[\cot\frac{\psi_o(\tau)}{2} - gz\right] \tag{15}$$

$$P(z,\tau) = P_o(\tau)\, A(z,\tau) \tag{16}$$

$$A(z,\tau) = A(z,\psi_o)$$

$$\equiv \left[1 - 2gz\sin\frac{\psi_o}{2}\cdot\cos\frac{\psi_o}{2} + g^2z^2\sin^2\frac{\psi_o}{2}\right]^{-1} \tag{17}$$

with $\psi_o(\tau) \equiv \psi(0,\tau)$ and $P_o(\tau) = \frac{1}{2\mu}\frac{\partial\psi_o}{\partial\tau}$. We shall restrict ourselves to this lossless case for which the complete pulse propagation behavior can be determined[8] from the modulating function $A(z,\tau)$.

The function $A(z,\tau)$ is plotted in Fig. XI-1 as a function of ψ_o for a fixed z. It is periodic in ψ_o with period 2π and contains a single maximum, as well as a single minimum, in each period. In the first period for $g < 0$ the minimum occurs at

$$\psi_m^- = \frac{\pi}{2} + \tan^{-1}\frac{|gz|}{2}, \qquad g < 0 \tag{18}$$

with corresponding minimum value A_m for $A(z,\psi_o)$

$$A_m = \left[1 + \frac{g^2z^2}{2}\left\{1 + \sqrt{1 + \frac{4}{g^2z^2}}\right\}\right]^{-1}. \tag{19}$$

The maximum occurs at

$$\psi_M^- = 2\pi - \tan^{-1}\frac{2}{|gz|}, \qquad g < 0 \tag{20}$$

with maximum value

$$A_M = \left[1 + \frac{g^2z^2}{2}\left\{1 - \sqrt{1 + \frac{4}{g^2z^2}}\right\}\right]^{-1}. \tag{21}$$

For $g > 0$, the maximum is at

$$\psi_M^+ = \tan^{-1}\frac{2}{gz}, \quad g > 0 \tag{22}$$

with value A_M and the minimum at

$$\psi_m^+ = \pi + \tan^{-1}\frac{2}{gz}, \quad g > 0 \tag{23}$$

with value A_m. The function $A(z,\psi_o)$ for the amplifier case (Fig. XI-1b) is indeed just a displacement of the attenuator case (Fig. XI-1a) by $2\psi_m^-$.

For small z, the difference between the values A_M and A_m is small. But as z increases A_M also increases monotonically while A_m decreases monotonically. For large z, A_m eventually becomes vanishingly small, whereas A_M becomes arbitrarily

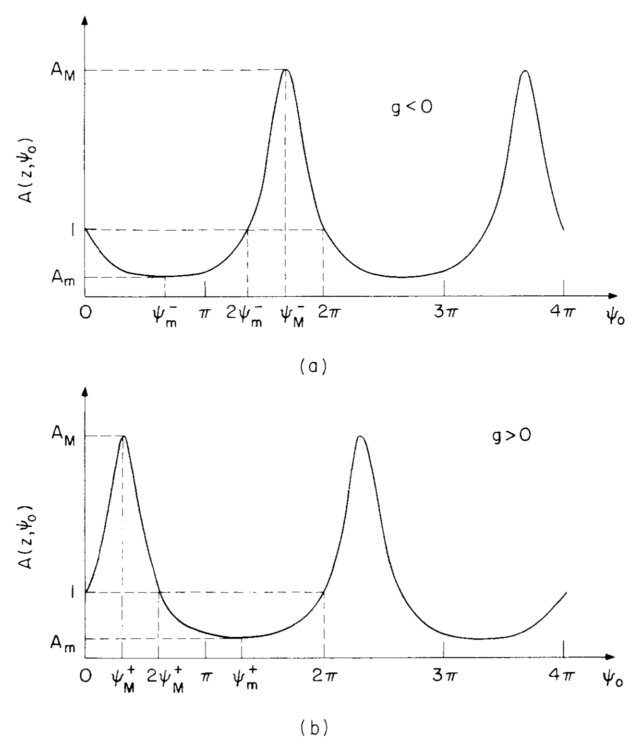

Fig. XI-1. (a) Behavior of the periodic $A(z,\psi_o)$ in a two-photon absorbing medium. Maximum and minimum parameters ψ_M^-, ψ_m^-, A_M and A_m are given by Eqs. 18-21. (b) Behavior of $A(z,\psi_o)$ for a two-photon amplifier with ψ_M^+, ψ_m^+ given by Eqs. 22 and 23.

large. In the first period the corresponding ψ_M^- moves to 2π and ψ_M^+ moves to 0. Thus a large pulse occupying several periods will break up into small pulses at large z. This is particularly easy to see from Fig. XI-1 for a square pulse where $\psi_o \propto \tau$. The physical mechanism of the sharpening is also clear. From Fig. XI-1a we see that energy is continuously extracted from the pulse front and fed back to the end of a 2π pulse.

The area under the $A(z,\psi_o)$ curve in each period is equal to an input energy $\psi(0) = 2\pi$ and, from (14), is a constant independent of z.

$$\int_{t_o}^{\infty} P(z,\tau)\, d\tau = \int_{t_o}^{\infty} P_o(\tau)\, d\tau = \int_0^{2\pi} A(z,\psi_o)\, d\psi_o = 2\pi. \tag{24}$$

From (24) and (17) it can be shown that as $z \to \infty$, the function $A(z,\tau)$ converges asymptotically to a sequence of δ-functions at τ_n determined by

$$\psi_o(\tau_n) = 2n\pi; \qquad n = 1, 2, \ldots, \quad g < 0, \tag{25}$$

from (17) or (20). An additional δ-function occurs at the pulse front $\psi_o(\tau_o) = 0$ for the amplifier case $g > 0$. Note that ψ_o is a positive monotone function of τ so that for any given $\theta(0) = \psi_o(\infty)$, there is at most one τ_n satisfying (25) for any n.

For an input pulse with a bounded support (i.e., a pulse that is only nonvanishing over a finite interval) these results imply the following general behavior of $P(z,\tau)$. For an arbitrary input area $\theta(0)$, the area theorem (14) for $\gamma = 0$ shows that at large z $\theta(0)$ will be reduced to the nearest $2p\pi$ in an absorbing medium and amplified to the nearest $2(p+1)\pi$ in an inverted medium for an integer p. In the limit, the pulse goes over to a δ-function pulse train given by

$$2\mu P(\infty,\tau) = 2\pi \sum_{n=1}^{p} \delta(\tau-\tau_n), \qquad g < 0 \tag{26a}$$

$$2\mu P(\infty,\tau) = 2\pi \sum_{n=0}^{p} \delta(\tau-\tau_n), \qquad g > 0 \tag{26b}$$

where τ_n are determined by (25). From the area theorem (14) the equilibrium values $\theta(0) = 2p\pi$ are unstable against a loss of 2π for $g < 0$ and unstable against a gain of 2π for $g > 0$, as illustrated in Fig. XI-2.

The pulse propagation behavior of a 4π sech input pulse of bounded support centered at $\tau = 0$ is plotted in Fig. XI-3 for a two-photon absorption medium. The breakup and sharpening of the pulse arise as expected from these results.

We shall not discuss the propagation of pulses with unbounded support. These pulses are unphysical as has been discussed for the one-photon case.[9] It might be mentioned, however, that even when these pulses are included the only solitary wave in two-photon absorption media is a 2π Lorentzian pulse that is unstable against loss, as shown in Fig. XI-2.

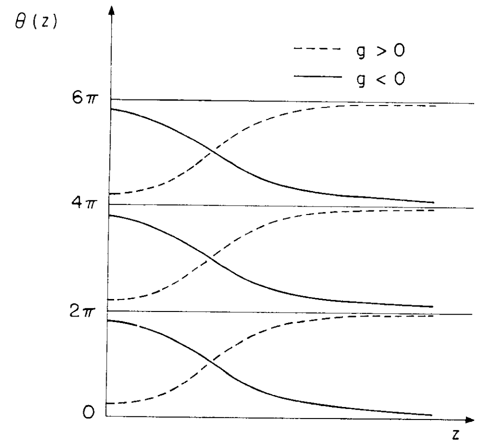

Fig. XI-2.
Behavior of the area θ(z), $\theta(z) = 2\cot^{-1}\left[\cot\frac{\theta(0)}{2} - gz\right]$, for two-photon attenuators and amplifiers from Eq. 14 with $\gamma = 0$.

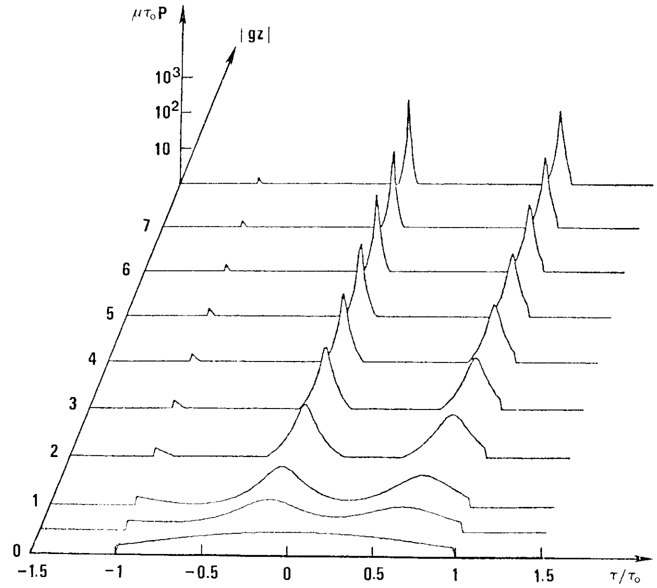

Fig. XI-3.
Formation of two sharp pulses at $\tau = 0$ and $\tau = \tau_o$ for a 4π input $2\mu P_o(\tau) = \frac{2\pi}{\tau_p}\frac{\text{sech}^2\tau/\tau_p}{\tanh\tau_o/\tau_p}$, $\tau_o \geq \tau \geq -\tau_o$, with $\tau_p = \tau_o$. Equations 16 and 17 are used for a two-photon absorption medium.

The present two-photon problem can be compared with the one-photon case as follows. Mathematically, only asymptotic solutions of the propagation equations that are sufficient for a long medium are generally available for one-photon ultrashort propagation.[2-6] A series of solitons[3-6] of finite width is obtained in the self-induced transparency problem.[2] On the other hand, our two-photon results apply to all lengths of the medium and exhibit the analytic behavior of the pulse breakup and continuous pulse sharpening. Ultrashort pulse propagation in one-photon amplifiers is unstable mathematically, which is also expected on physical grounds from the onset of stimulated emission or self-oscillation, while the pulse-sharpening characteristic in a two-photon amplifier is not altered by perturbation, as can be shown by the exact solution (16). This behavior may prevail in an actual physical situation because the two-photon medium is stable against spontaneous oscillation, and one-photon emission between the two levels is forbidden by parity. Obviously, the slowly varying envelope approximation and even the optical medium model with or without loss break down when the pulse becomes too short.

These results suggest that short pulses of $\Delta\tau \sim 10^{-14}$ s duration may be generated by passing a ps pulse through a two-photon absorption medium. A great many useful two-photon adsorption media have been reported in recent works on two-photon absorption.[10] We expect to give a detailed discussion of material systems suitable for two-photon pulse shortening in a future report. The effects of loss, inhomogeneous broadening, and self-focusing in two-photon ultrashort propagation are being investigated at present, as well as the mathematical solution of the original coupled Maxwell and material equations by the inverse method[4-6] and the existence of the two-photon equivalent of breathers.[5]

The authors wish to thank Professor H. A. Haus and Professor R. S. Kennedy for helpful discussions. Professor Chu's research is supported by funds from the Dugald C. Jackson Professorship of the Department of Electrical Engineering and Computer Science.

References

1. H. P. Yuen, Appl. Phys. Letters 26, 505 (1975).
2. S. L. McCall and E. L. Hahn, Phys. Rev. 183, 457 (1969).
3. G. L. Lamb, Jr., Rev. Mod. Phys. 43, 99 (1971).
4. G. L. Lamb, Jr., Phys. Rev. Letters 31, 196 (1973).
5. M. J. Ablowitz, D. J. Kaup, and A. C. Newell, J. Math. Phys. 15, 1852 (1974).
6. A. C. Scott, F. Y. F. Chu, and D. W. McLaughlin, Proc. IEEE 61, 1443 (1973).
7. See the detailed discussion of two-photon spectroscopy by J. M. Worlock, in F. T. Arecchi and E. O. Schulz-DuBois (Eds.), Laser Handbook, Vol. II (North-Holland Publishing Company, Amsterdam, 1972), p. 1323.
8. After the present work was completed the authors learned that Eq. 16 had been obtained previously by L. E. Estes, L. M. Narducci, and B. Shammas, Nuovo Cimento Letters 2, 775 (1971); I. A. Poluektov, Yu. M. Popov, and V. S. Roitberg, JETP Letters 18, 373 (1973).
9. A. Icsevgi and W. E. Lamb, Jr., Phys. Rev. 185, 517 (1969).
10. See D. Pritchard, J. Apt, and T. W. Ducas, Phys. Rev. Letters 32, 641 (1974); M. D. Levenson and N. Bloembergen, Phys. Rev. Letters 32, 645 (1974); P. F. Liao and J. E. Bjorkholm, Phys. Rev. Letters 34, 1 (1975); and references cited therein.

C. LOWER BOUND TO THE ERROR PROBABILITY FOR QUANTUM DETECTION OF M PURE STATES

National Aeronautics and Space Administration (Grant NGL 22-009-013)

Nam-Soo Myung

In RLE Progress Report No. 117 (pp. 267-271), we determined a lower bound to the average error probability for detecting M quantum signals in which each signal state occurs with probability p_i and has density operator ρ_i. The lower bound is given by

$$P_e \geq \frac{1}{2}\left[\sum_{i=1}^{M}\left(p_i + (1-p_i)\sum_{k:\xi_k(i)<0}\xi_k(i)\right)\right], \tag{1}$$

where $\sum\limits_{k:\xi_k(i)<0} \xi_k(i)$ represents the sum of the negative eigenvalues of the operator

$$\sum_{\substack{j=1\\ j\neq 1}}^{M} \frac{p_j}{1-p_i}\rho_j - \frac{p_i}{1-p_i}\rho_i. \tag{2}$$

In the first part of this report, we shall simplify this bound, and then (1) can be determined relatively easily for the pure state problem. In the second part, we shall present some physical interpretations of the lower bound by comparing it with the classical detection problem.

1. Linearly Independent Pure State Problem

When every signal state is a pure state

$$\rho_i = |s_i\rangle\langle s_i| \tag{3}$$

and the eigenvalue problems associated with (1) are relatively simple. The problem reduces to that of finding the negative eigenvalues and eigenvectors for

$$\left[\sum_{\substack{j=1\\ j\neq i}}^{M} \frac{p_j}{1-p_i}|s_j\rangle\langle s_j| - \frac{p_i}{1-p_j}|s_i\rangle\langle s_i|\right]|\xi(i)\rangle = \xi(i)|\xi(i)\rangle \qquad \text{for } i = 1, \ldots, M. \tag{4}$$

Our first step will show that for every i there is only one negative eigenvalue of (4); hence, we need only investigate i = 1. In attacking this problem, we assume that the $|s_i\rangle$ are linearly independent, and base the problem on the M-dimensional Hilbert space that they span. For i = 1, Eq. 4 is equivalent to

$$\left(\sum_{j=2}^{M} p_j |s_j\rangle\langle s_j| - p_1|s_1\rangle\langle s_1|\right)|\xi\rangle = (1-p_1)\,\xi|\xi\rangle. \tag{5}$$

For simplicity, we have used ξ in (5) instead of $\xi(1)$. Multiplying both sides of (5) by $\langle s_k|$ yields

$$\sum_{j=2}^{M} p_j\langle s_k|s_j\rangle\langle s_j|\xi\rangle - p_1\langle s_k|s_1\rangle\langle s_1|\xi\rangle = (1-p_1)\,\xi\langle s_k|\xi\rangle, \qquad \text{for } k = 1,\dots M, \tag{6}$$

or in matrix form

$$\begin{bmatrix} \langle s_1|s_1\rangle, \dots, \langle s_1|s_M\rangle \\ \vdots \\ \langle s_M|s_1\rangle, \dots, \langle s_M|s_M\rangle \end{bmatrix} \begin{bmatrix} -p_1 & & & \\ & p_2 & & \\ & & \ddots & \\ & & & p_M \end{bmatrix} \begin{bmatrix} \langle s_1|\xi\rangle \\ \vdots \\ \langle s_M|\xi\rangle \end{bmatrix} = (1-p_1)\xi \begin{bmatrix} \langle s_1|\xi\rangle \\ \vdots \\ \langle s_M|\xi\rangle \end{bmatrix}. \tag{7}$$

Let U be the $M \times M$ matrix whose elements are $\langle s_i|s_j\rangle$. The matrix U is a Hermitian matrix that always has real eigenvalues. Thus the determinant of U, which is the product of eigenvalues, is also real. Every diagonal element of U is equal to 1 because every $|s_i\rangle$ is a unit vector. The matrices formed by the inner products of a set of vectors, like U, are called Gram matrices.[1] If the set of vectors is linearly independent, the Gram matrix has a positive determinant. This implies that U is positive-definite, since any Gram matrix of a subset of a set of linearly independent vectors also has a positive determinant. Furthermore, the determinant of a Gram matrix of a smaller subset of vectors has a determinant greater than or equal to that of a larger subset of vectors. Let U_1 be a $(M-1)\times(M-1)$ matrix whose elements are $\langle s_i|s_j\rangle$ for $i,j = 2,\dots,M$. Then

$$0 < (\det U)/(\det U_1) \leq 1 \tag{8}$$

is true. Since U is positive-definite, U^{-1} always exists and is also positive-definite. If we denote $U^{-1}_{i,j}$ by i, j elements of U^{-1}, then (for further details see Gantmacher[1])

$$U^{-1}_{1,1} = (\det U_1)/(\det U). \tag{9}$$

Now let us turn to the problem of finding the number of negative eigenvalues. For simplicity, let

$$P_1 = \begin{bmatrix} -p_1 & & . & . & . & 0 \\ & p_2 & & & 0 & . \\ . & & p_3 & & & . \\ . & 0 & & \ddots & & \\ 0 & . & . & . & & p_M \end{bmatrix}. \tag{10}$$

Equation 7 can be written

$$P_1\underline{d} = \lambda U^{-1}\underline{d}, \tag{11}$$

where $\underline{d}$ is a column vector whose elements are $\langle s_i | \xi \rangle$, and $\lambda = (1-p_1)\xi$. This is called the generalized eigenvalue equation.[2] Since U^{-1} is a positive-definite matrix, there always exist[2] M real positive eigenvalues $\lambda_1, \ldots, \lambda_M$. Without loss of generality, let

$$\lambda_1 \leqslant \lambda_2 \leqslant \ldots \leqslant \lambda_M. \tag{12}$$

Consider another generalized eigenvalue equation given by

$$\tilde{P}_1\tilde{\underline{d}} = \tilde{\lambda}U^{-1}\tilde{\underline{d}}, \tag{13}$$

where $\tilde{P}_1$ is the $M \times M$ diagonal real matrix

$$\tilde{P}_1 = \begin{bmatrix} 0 & . & . & . & . & .0 \\ 0 & p_2 & & & & . \\ & & p_3 & & & . \\ . & & & . & & . \\ . & & & & . & 0 \\ 0 & . & . & . & .0 & p_M \end{bmatrix}.$$

The matrix equation (13) also has M real eigenvalues that can be ordered so that

$$\tilde{\lambda}_1 \leqslant \tilde{\lambda}_2 \leqslant \ldots \leqslant \tilde{\lambda}_M. \tag{14}$$

The difference between P_1 and $\tilde{P}_1$ is that the first diagonal element of P_1 is replaced by zero. Thus $\tilde{P}_1 - P_1$ is nonnegative-definite and has rank one. This implies that the eigenvalues λ and $\tilde{\lambda}$ are interlaced as follows.[2]

$$\lambda_1 \leqslant \tilde{\lambda}_1 \leqslant \lambda_2 \leqslant \tilde{\lambda}_2 \leqslant \ldots\ldots \leqslant \lambda_M \leqslant \tilde{\lambda}_M. \tag{15}$$

The minimum eigenvalue, λ_1, of (13), can be determined from

$$\tilde{\lambda}_1 = \min_{\underline{d}\neq\underline{0}} \frac{\underline{d}^\dagger\tilde{P}_1\underline{d}}{\underline{d}^\dagger U^{-1}\underline{d}} = 0. \tag{16}$$

Consequently the minimum eigenvalue of $\tilde{\lambda}_1$ is nonpositive and other eigenvalues are nonnegative. Moreover,

$$\lambda_1 = \min_{\underline{d}\neq\underline{0}} \frac{\underline{d}^\dagger P_1 \underline{d}}{\underline{d}^\dagger U^{-1} \underline{d}}. \tag{17}$$

Therefore, for the pure state problem, the lower bound to the average error probability is given by

$$P_e \geq \frac{1}{2}\left[1 + \sum_{i=1}^{M} (1-p_i)\xi_i\right], \tag{18}$$

where ξ_i is the <u>only</u> negative eigenvalue of

$$\sum_{\substack{j=1\\ j\neq i}}^{M} \frac{p_j}{1-p_i} |s_j\rangle\langle s_j| - \frac{p_i}{1-p_i} |s_i\rangle\langle s_i|, \tag{19}$$

and is given by (17) with $\lambda_i = (1-p_i)\xi_i$.

References

1. F. R. Gantmacher, Matrix Theory, Vol. 1 (Chelsea Publishing Co., Bronx, New York, 1960), pp. 242-293.

2. Ibid., pp. 310-326.